Original Article
Cite This: Colloid & Nanoscience Journal 1 (2023) 16-25.
CNJ.araku.ac.ir

Effect of composition, electrolyte pH, annealing temperature and electrodeposition waveform on the magnetic properties of Co-Cu nanowire alloys

Mojgan Najafi,[1*] Ramin Gholamhosseiny[2]

Received:2023-01-16
Revised: 2023-02-07
Accepted: 2023-02-08
DOI: 10.52547/CNJ.1.1.16

[1]Department of Materials Engineering, Hamedan University of Technology (HUT), Hamedan, Iran

[2]Department of Physics, Faculty of Science, Bu-Ali Sina University, P.O.Box 65174, Hamedan, Iran

Abstract

Arrays of $Co_{0.2}Cu_x$, with $0<x<0.1$, nanowires (NWs) have been synthesized. CoCu NWs have been grown into the AAO templates by ac electrodeposition. The anodic aluminum oxide template (AAO) was synthesized by a two-step anodization process of pure Al foils in sulfuric acid. The effect of the small addition of Cu to Co NWs by varying the concentrations of Cu^{2+} ions in the electrolyte, as well as the effect of annealing on the magnetic properties of NWs, was investigated. Eventually, the effect of changing waveforms applied to nanowire deposition was studied. The results showed that the coercivity of cobalt NWs decreased by adding copper impurity as a non-magnetic material from 1337 Oe to 660 Oe. By annealing of the alloy NWs up to 450 °C, the coercivity increases from 1140 Oe value for pure Co NWs up to 1541 Oe for CoCu NWs due to the removal of structural stresses of the nanowire.

Keywords: CoCu alloys, Thermal annealing, Electrodeposition, Anodic aluminum oxide (AAO) templates

1. Introduction

Recently, much research has been done on nanowires (NWs) and nanotubes of metals and semiconductors because of their unique physical properties. Manufacturing nanometer-sized wires are both technologically and scientifically attractive because nanometer-sized devices exhibit unusual properties. The ratio of length to the diameter of NWs is very high. These wires have a variety of applications in the fields of nano-electronics [1], optics [2], various gas sensors [3], and magnetic memory [4, 5]; due to their interesting properties. The NWs are anisotropic one-dimensional structures with a small diameter and a high surface-to-volume ratio, therefore, their properties are different from other structures. In recent years, advances in the field of magnetism and magnetic materials, the synthesis and fabrication of magnetic NWs through their unique magnetic properties have attracted increasing attention and opened many perspectives to the field of magnetic science. The metallic magnetic NWs show very square shape hysteresis loops, which makes these NWs as a very good candidate for magnetic data storage [6-8]. It is well known that the addition of non-magnetic impurities to ferromagnetic NWs can greatly improve their magnetic properties [9-12]. Among the various methods for the preparation of NWs, including lithography [13], sputtering [14, 15], vapor deposition [16], molecular beam epitaxy (MBE) [17], template-assisted electrodeposition is a popular way to obtain a uniform, highly ordered NW arrays and has been shown to be one of the simplest and most inexpensive easily controlled methods [9-12, 18-23]. On the other hand, the properties of electrodeposited NWs in AAO templates can be controlled by several factors; such as current density, electrolyte composition, time of deposition, temperature, reduction potential (different for each material), pH, microstructure peculiarities etc. Many arrays of magnetic NWs including Fe [24], Co [25], Ni [26], and their alloys [27-29] have been prepared via AAO assisted electrodeposition method. Although, there have been numerous publications about ferromagnetic–nonmagnetic alloy NW arrays such as CoPd [30], CoAg [31], FeAg [31], CoPb [32], and CoPt [33] deposited in AAO template, CoCu NW arrays system has been scarcely reported in the literature. The addition of nonmagnetic elements to magnetic elements is one of the most common and effective ways to tune of structural and magnetic properties of magnetic NWs [11]. Although many articles have been published on magnetic and non-magnetic alloys, due to their interesting magnetic and magnetotransport properties, however, no systematic study has been performed on factors.

Corresponding Author: Mojgan Najafi
E-mail address:
mojgannajafi1@gmail.com

In the present study, the synthesis of CoCu NWs in AAO templates is performed at room temperature using AC potentials from -15 to +15 V, as well as changing electrolyte composition (Co^{++}/Cu^{++} concentration ratio) to change the structural and magnetic properties. Also, the effect of pH, AC potential waveform and annealing temperature of deposited NWs on the magnetic properties of synthesized NWs have been investigated.

2. Experimental

2.1. Material

All chemicals containing cobalt sulfate ($CoSO_4.H_2O$), copper sulfate ($SnSO_4$), Sodium gluconate ($C_6H_{11}NaO_7$), boric acid (H_3BO_3), phosphoric acid (H_3PO_4), chromic acid (H_2CrO_4), sulfuric acid (H_2SO_4), perchloric acid ($HClO_4$), ethanol (C_2H_5OH), sodium hydroxide (NaOH) and aluminum foil (99.99%) were purchased from Merck and Sigma-Aldrich companies and used without further purification. All aqueous solutions were prepared using double distilled water. In all experiments, the temperature was controlled to within 0.1 °C by circulating thermostated water through the jacketed glass cell, and the sample solution was continuously stirred by a magnetic stirrer.

2.2. CoCu nanowires (NWs) preparation

CoCu NW fabrication consists of two parts: 1) fabrication of anodic aluminum oxide (AAO) template by two-step anodizing; and 2) deposition of a solution containing Co and Cu ions into the template by electrodeposition method. Anodic aluminum oxide (AAO) as a template for the synthesis of CoCu alloy NW arrays was prepared by the two-step optimized anodization process, as reported in the literature [9-12, 34, 35]. High-purity aluminum sheets (99.99%) with a thickness of 3 mm were refined by electropolish in a mixture of perchloric acid and ethanol in a ratio of 1:4. They were then anodized in a constant DC voltage of 25 V at 4 °C in 0.3 M aqueous solution of sulfuric acid for 7 h. The oxide layer was then removed by a mixture of 0.5 M H_3PO_4 and 0.3 M CrO_3 at 40 °C for 24 hours. Finally, the second anodization is performed in conditions similar to those of the primary anodization for 30 min. At the end of the second anodization, a barrier layer of Al_2O_3 on the bottom of the pores is estimated to be about 25 nm. This barrier layer is too thick and is thinned for the electrodeposition of NWs [36].

Self-ordered CoCu NWs array with 25 nm diameter using two standard electrode cells (AAO template and platinum plate) using sine wave alternating voltage and 30 V_{pp} voltage and 200 Hz frequency for 3 min were fabricated. In order to synthesize at different NWs diameters, the template was synthesized by oxalic acid as anodizing electrolyte. Briefly, the first stage anodizing conditions were performed for 24 h in 0.3 M oxalic acid at 4 °C under 40 V DC potential. After etching for 24 hours in a solution containing 0.2 M chromic acid and 0.5 M phosphoric acid at 50 °C. The anodize conditions of the second stage were the same as the first anodization condition for 20 hours. Then, the aluminum behind the samples was removed with $CuCl_2.2H_2O$ (0.1 M) and HCl (1.64 M) solution and only the aluminum oxide layer remained. The diameter of the pores was increased using a phosphoric acid solution (5%) at 32 °C. Then a layer of gold was sputtered on the back of the prepared AAO. The electrolyte contains an aqueous bath of varying concentrations of $CoSO_4$ and $CuSO_4$, and H_3BO_3 as a buffer was used for the electrodeposition of ions (see Table 1). After fabricating the NWs, the NWs were annealed in argon gas atmospheres for 20 minutes at different temperatures, ranging from 300 to 55.0 °C, and then cooled slowly to room temperature. SEM images were used to characterize and study the morphology of nanopores and NW arrays. The magnetic properties of the as-synthesized after-annealedaled NWs were measured by the alternating gradient force magnetometer (AGFM) the room temperature.

Table 1. Materials and concentrations of electrolyte solutions

Salt name	Molarity	Sample name
$CoSO_4.7H_2O$	0.2 M	
$CuSO_4.5H_2O$	(0.001, 0.01, 0.04, 0.08, 0.1) M	$Co_{0.2}Cu_x$ (x= 0, 0.001, 0.01 ,0.04, 0.08, 0.1)
H_3BO_3	0.5 M	

2.3. Characterization

The morphology of the AAO template and nanowires was examined by field-emission scanning electron microscopy (FESEM; MIRA3 TESCAN) after dissolving the template in an aqueous solution of 3 mol L^{-1}

NaOH. The Crystal structure of nanowires using X-ray diffraction (XRD; Philips X'Pert Pro; Cu Kα radiation; λ = 0.154 nm) was investigated. For XRD analysis, the back of the template was eliminated with a saturated $CuCl_2$ solution. To investigate the magnetic properties, major hysteresis loops using vibrating sample magnetometer (VSM; MDKB) were obtained at room temperature.

3. Results and discussion

3.1. SEM analysis

Fig. 1 shows the SEM image of the NWs, after they were removed from the AAO template. It can be seen that the NWs have an approximate 25 nm in diameter and several micrometers in length, which corresponds to the size of the AAO templates.

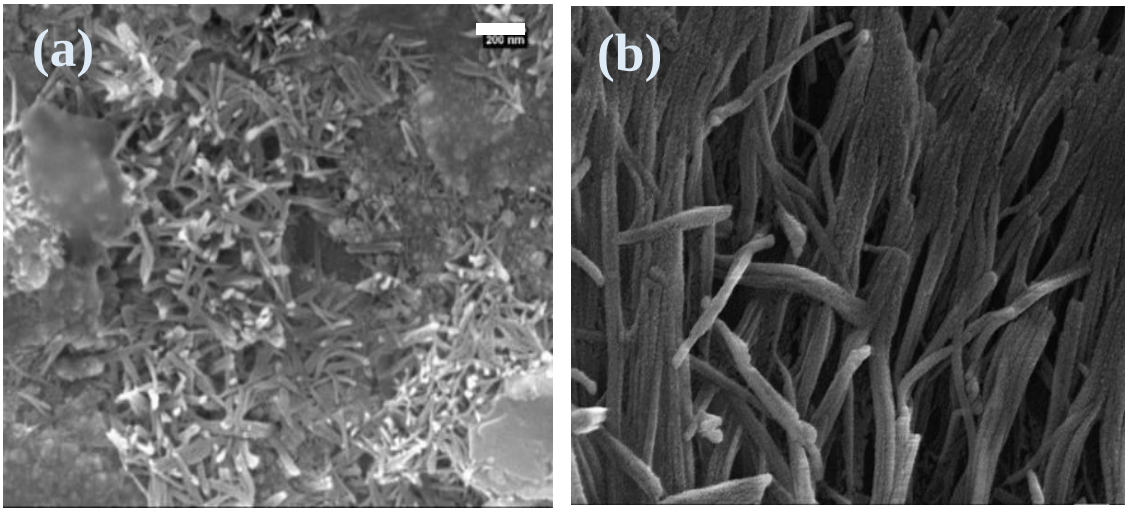

Fig. 1. SEM image of cobalt-copper alloy nanowires after the release of the template with two different magnifications. ((a) Scale bar is 200 nm).

3.2. XRD analysis

Fig. 2 shows the diffractograms for the synthesized Co–Cu nanowires. The XRD spectrum of the electrodeposited nanowires has a high copper dominance by the appearance of a very intense peak of fcc Cu (111) and a peak of medium intensity for fcc Cu (200) as reported in JCPDS n° 04-0836. In addition, we have observed a small peak of hcp Co (100). From the XRD results, we noted that Co–Cu nanowires have a polycrystalline structure. The alumina peaks are indexed by exploiting the standardXRDdata (JCPDS n° 10-173).

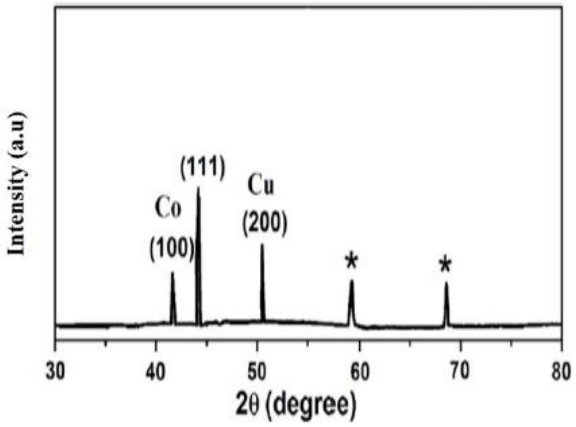

Fig. 2. XRD patterns for the electrodeposited Co–Cu nanowires.
(* denoted for the alumina, Al_2O_3, peaks).

3.3. VSM analysis

Fig. 3 shows the hysteresis loops of arrays of CoCu NWs (synthesized using Co^{++}=0.2 M and different Cu^{++} concentrations) in the template by applying the field along the NWs. As can be observed, all of the loops have a nearly square shape due to the demonstration of strong shape anisotropy. It is evident that the easy axis of magnetization is along the NWs but the decrease in the loop area is due to the reduction of the saturation magnetization of the NWs by adding non-magnetic Cu material. In all of these NWs with different percentages of copper, shape anisotropy along the NWs is the dominant effect on their magnetization and the easy axis of magnetization is along the NWs.

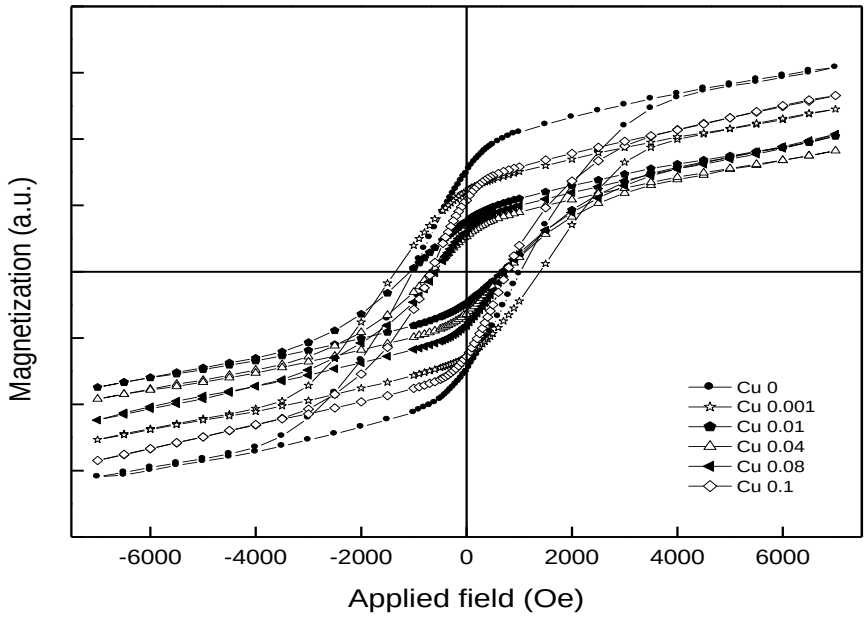

Fig. 3. Hysteresis loops of electrodeposited nanowires with different Cu^{++} concentrations in electrodeposition solution; Co^{++}(0.2 M)/Cu^{++} (x M; x= 0, 0.001, 0.01, 0.04, 0.08, 0.1).

Fig. 4a shows a plot of the coercivity of the samples against the concentration of Cu in NWs. However, with the addition of up to 0.01 M copper, the coercivity decreases, but wa with a further increase in copper content (up to 0.1 M) the coercivity remains almost constant and changes slightly. The coercivity of the samples decreases with the addition of copper impurities from 1337 Oe to 660 Oe. The decrease in coercivity with increasing non-magnetic impurity has been reported previously [12,37]. According to the symmetric fanning model, the coercivity of NWs decreases with the increase of the nonmagnetic content [38-40].

Also, atomic absorption spectroscopy (AAS) was used to determine the composition of $Co_{0.2}Cu_x$ NWs after the release of the template, and the results are tabulated in Table 2. The results of the AAS analysis of NWs show that the percentage of copper in the NW reaches 36 (% mole ratio) with increasing molar concentration of Cu^{++} in the electrodeposition bath to 0.01 M and with the addition of more copper salt concentration, the percentage of copper in the NW is slightly increased. In other words, with an increasing molar percentage of copper salt (more than 0.01 M) in the solution, the percentage of copper in the synthesized alloy NW remains almost constant. Therefore, it is expected that the coercivity will remain constant in NWs with more than 36 (%mole ratio) copper (Fig. 4a).

In order to improve the magnetic properties, the samples were annealed. As can be seen in Fig. 4b, the coercivity of the whole sample is improved by annealing, because of slowly improvement of the crystalline structure of NWs with annealing and cooling slowly in inert an atmosphere. The anomalies and dislocations in the crystal structure created during the rapid accumulation of NWs have been reduced by annealing. By annealing alloy NWs to relieve the structural stresses, the coercivity increases for pure and alloy NWs. Figure 3 shows that for the pure cobalt sample, the coercivity increases from 1308 Oe at 300 °C to 1540 Oe at 550 °C. The same increase for the $Co_{0.64}Cu_{0.36}$ alloy sample increases from 700 Oe to 980 Oe was observed.

Table 2. Analysis of atomic absorption spectroscopy at different copper concentrations

Salt name	% Cu in nanowire composition	% Co in nanowire composition

0.001	Cu	12	88
0.01	Cu	36	64
0.08	Cu	52	48
0.1	Cu	58	42

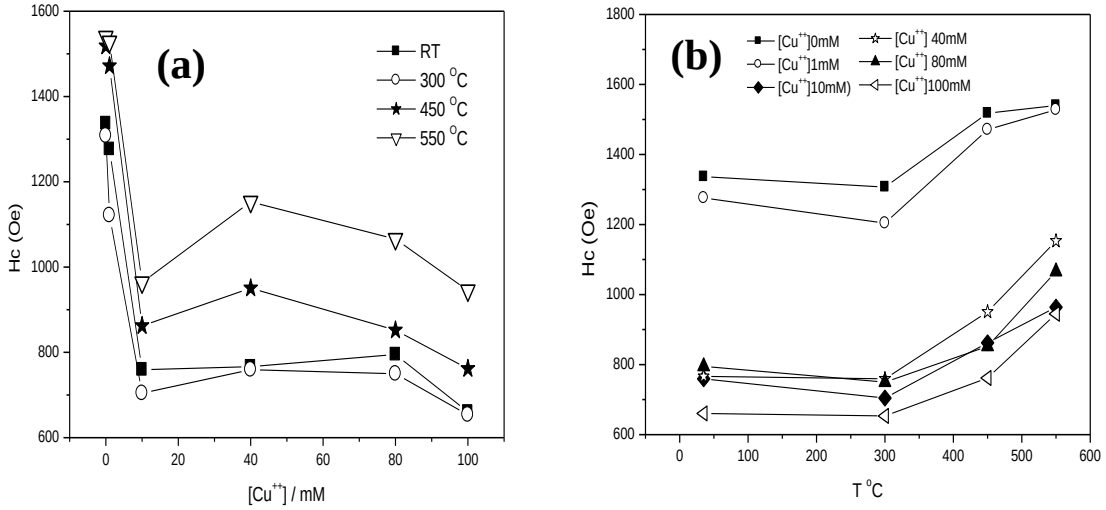

Fig. 4. The coercivity of Co-Cu nanowires, measured with the field applied parallel to the nanowires as a function of the (a) composition of deposition electrolyte; and (b) annealing temperature.

To investigate the effect of the waveform on the magnetic properties of the NWs, a sample solution with Co^{++}/Cu^{++}=0.2/0.01 was used for the synthesis of NW at 200 Hz. It was performed by three types of sine, square, and triangular electrodeposition waveforms. Fig. 5 shows a comparison between the coercivity of as pras-preparedusing different electrodeposition waveforms before and after annealing at 450 °C. All three samples are synthesized from the same electrodeposition solution and only have different electrodeposition waveforms. Fig. 5 shows that the coercivity in the specimen made with the square and triangular waveforms is significantly greater than that made with the sinusoidal waveform. Also, the AAS results demonstrate that for a typical concentration ratio of Co to Cu ions in solution (0.2:0.01), the percentage of metals in the NWs changes with the electrodeposition waveforms. In the samples made with square and triangular waveforms, the percentage of cobalt is significantly higher than that made with sinusoidal waveforms. The coercivity of all three specimens increased after annealing, which could be due to stress relief in the NW structure.

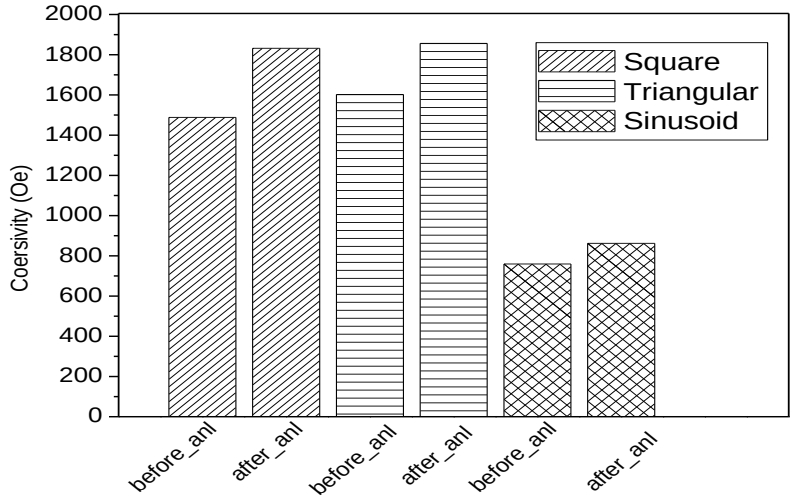

Fig. 5. The coercivity of synthesized nanowire with $[Co^{++}]:[Cu^{++}]$ = 0.2:0.01 by different electrodeposition wavefwaveformsre and after annealing at 450 °C.

The pH values of the electrolyte bath were vertically in the range of 2 to 2.5. To investigate the effect of pH on the magnetic properties of Co-Cu NW alloys, the pH of the solution was increased up to 6, by the addition of NaOH to the electrolyte solution for a typical sample ($[Co^{++}]/[Cu^{++}]$=0.2/0.01). Three samples of

0.2 M Co^{++} and 0.01 M Cu^{++} concentration at pH=3, 4, 6 were electrodeposited at 200 Hz with sinusoidal waveform at room temperature for 5 min. Fig. 6a illustrates the hysteresis loops of fabricated NWs at different pH. The magnetic properties of the samples including the coercivity and squareness were calculated and plotted using corresponding hysteresis loops (Fig. 6 b). The highest coercivity is observed for the sample prepared at pH=3 which is equal to 759 Oe. Also, the squareness value was highest at this pH and measured to be 0.61. As shown in 6b, the magnetic properties of the samples decrease with increasing pH.

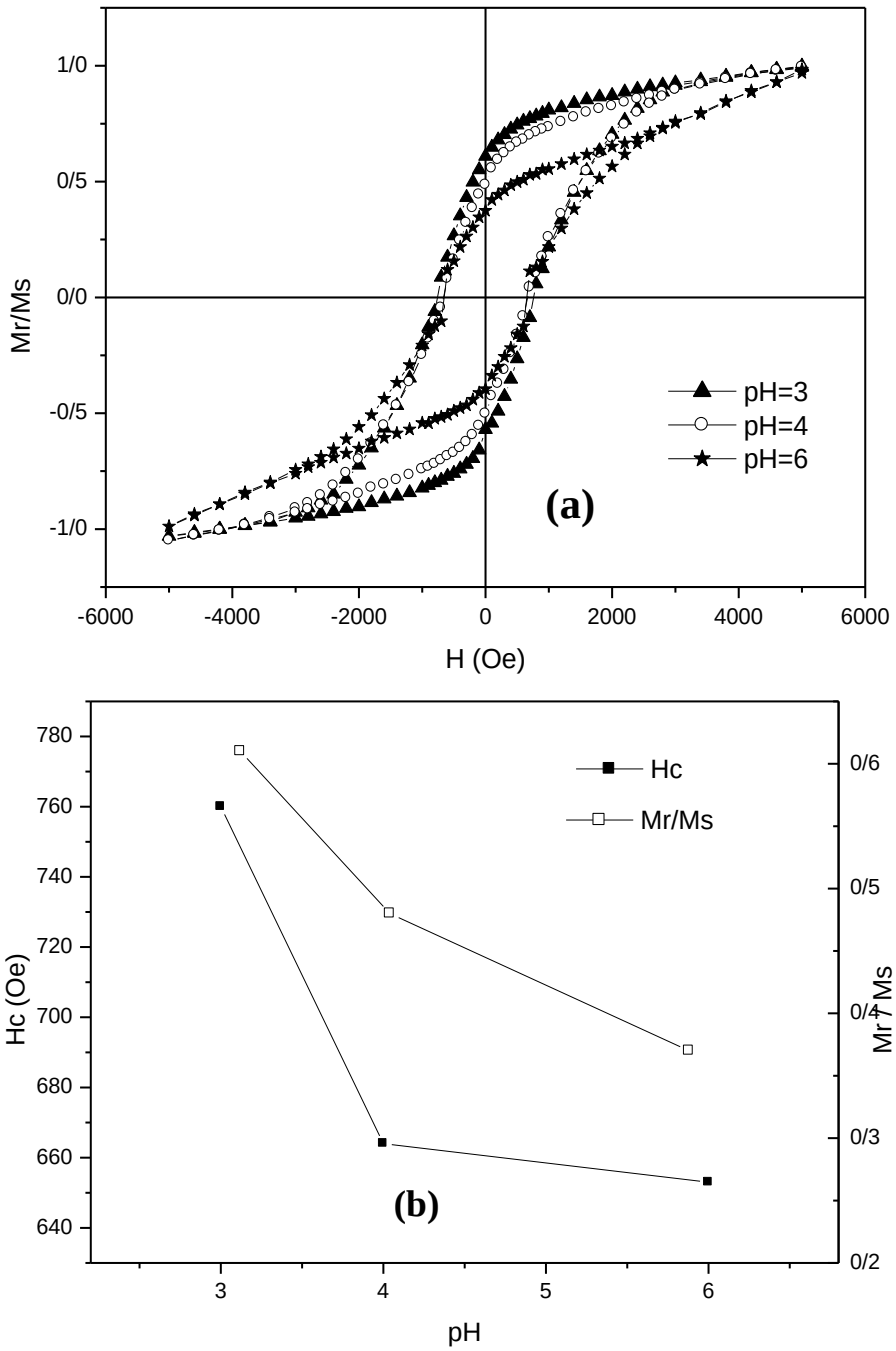

Fig. 6. (a) The hysteresis loops; (b) the H_C and S_q for a typical sample ($Co_{0.64}Cu_{0.36}$) nanowire as a function of pH.

This decrease in magnetic properties can be due to two phenomena: (a) an increase in Cu electrodeposition compared to Co in NWs which can directly reduce the magnetic properties of NWs; (b) a change of cobalt crystal structure from hcp at low pH (lower than 3) to both crystalline phases (hcp and fcc structure) at higher pHs [41]. Also, there is competition between shape anisotropy and crystalline magnetic

anisotropy that can control magnetic properties. Therefore, the decreasing behavior of magnetic properties is the result of all these factors. Increasing the pH somehow alters the crystal structure of the NWsthet hard axis of the magnetocrystalline anisotropy directions of the cp structure aligning the NW axis and decreasing the magnetic properties of NW [37]. Increasing the pH somehow alters the crystal structure of the NWs on the hard axis of the magnetocrystalline anisotropy directions of the cp structure aligning the NW axis and decreasing the magnetic properties of NW [37].

To investigate the effect of the diameter of NWs, we use DC electrodeposition in the templates with different pore diameters ranging from 50-70 nm. After the anodization process, the remaining Al layer is chemically removed. Then the barrier layer was etched with H_3PO_4 solution at room temperature. To widen the pore diameter, the templates were immersed in an H_3PO_4 solution for different periods of time. After that, a thin gold layer was sputtered on one side of the templates, and then gold was deposited at the bottom of the ores from Oreson's solution to physically bind the gold layer to the NWs. Nanowire deposition was carried out in a two-electrode cell using a Watts-type bath of $[Co^{++}]/[Cu^{++}]=0.2/0.01$ solutions at -1.5 V. The deposition time was 5 minutes at room temperature. The magnetic properties of the deposited NWs by different diameters are shown in Fig. 7. It can be seen that as the NW diameter increases, the coercivity and squareness decrease The coercivity decrease with increasing Co NWs diameter can also be attributed to several effects. The multi-domain formation in the NWs and increasing the magnetostatic coupling among the NWs with larger diameters are responsible for the variation of the coercivity in Fig. 7.

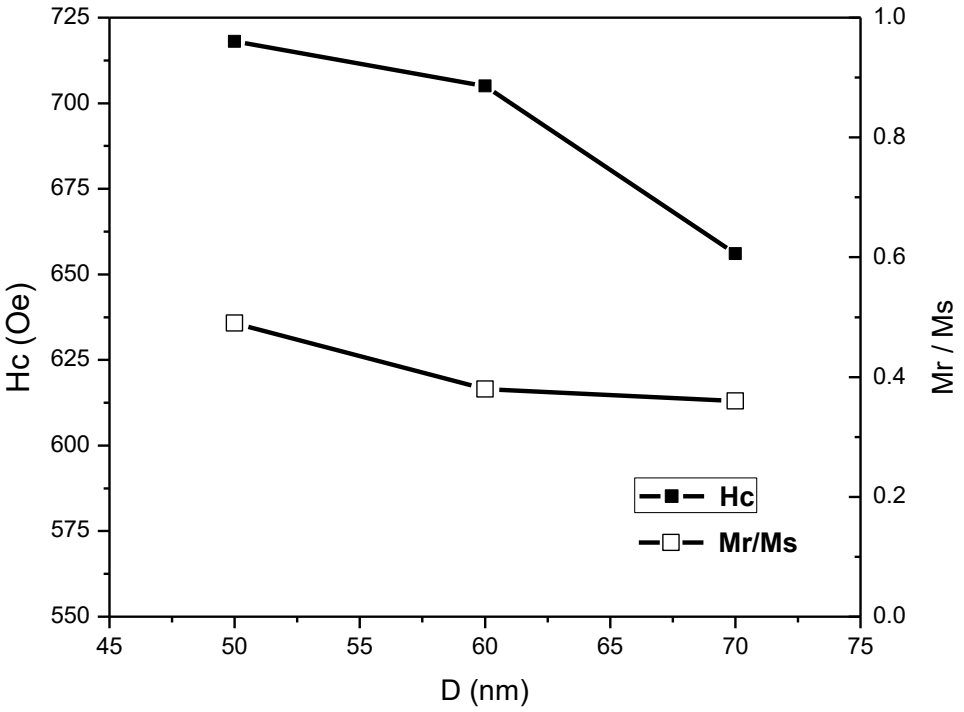

Fig. 7. The coercivity and squareness for a typical sample ($Co_{0.64}Cu_{0.36}$) nanowire as a function of nanowire diameters.

4. Conclusion

Pure Co and $Co_{100-x}Cu_x$ ($0 \leq x \leq 58$) alloy NW arrays have been fabricated by AC electrodeposition into the highly ordered homemade synthesized AAO templates. The effect of various Cu contents, pH, electrodeposition waveform, annealing temperature, and diameter of NWs on magnetic properties and structure of fabricated NWs were investigated by AAS, SEM, and AGFM. By varying the Cu^{++} concentration in the electrodeposition electrolyte solution, the amount of Cu in CoCu NWs has been tuned in the range of 0 up to ~58%. The magnetic properties of the NWs along the NWs axis show a decrease in coercivity and squareness with increasing copper impurity. Also, the magnetic properties of the fabricated NWs improved with increasing annealing temperature for pure cobalt NW and all of the $Co_{100-x}Cu_x$ alloy NWs. After annealing, both H_c squareness ness increased for rangesange of compositions and various annealing

temperatures which were due to crystal anisotropy changes. Typically, the H_c of $Co_{64}Cu_{36}$ NWs increase from 766 Oe to 1153 Oe after annealing at 550 °C. The coercivity of the NWs was investigated by chain ranges electrodeposition waveforms and the H of the electrolyte bath. The effect of pore diameter on the magnetic properties of $Co_{64}Cu_{36}$ NWs was investigated.

Conflicts of Interest

The author declares no conflict of interest.

Acknowledgments

The authors greatly acknowledge Hamedan University of Technology (HUT) for the financial support from the Grant Research Council.

Author information

*Corresponding Author:
E-mail address: mojgannajafi1@gmail.com

ORCID
Mojgan Najafi: 0000-0003-1690-6176

References

[1] H.-M. Hoang, T.-H. Duong, N.-H. Tran, H. Seo, J.W. Kim, J.Y. Kim, H.C. Kim, Synthesis of brass nanowires and their use for organic photovoltaics, Mater. Chem. Phys., 246 (2020) 122852. https://doi.org/10.1016/j.matchemphys.2020.122852.
[2] R.J. Wang, L. Chen, S. Tai, X.G. Deng, P.F. Sciortino, J.D. Deng, F. Liu, Wafer-based nanostructure manufacturing for integrated nanooptic devices, J. Lightwave Technol. 23 (2005) 474-485. https://doi.org/0.1109/JLT.2004.842298.
[3] Q. Wan, Q.H. Li, Y.J. Chen, T.H. Wang, X.L. He, J.P. Li, C.L. Lin, Fabrication and ethanol sensing characteristics of ZnO nanowire gas sensors, Appl. Phys. Lett. 84 (2004) 3654-3656. https://doi.org/10.1063/1.1738932.
[4] M. Al Bahri, Controlling domain wall thermal stability switching in magnetic nanowires for storage memory nanodevices, J. Magn. Magn. Mater. 543 (2022) 168611. https://doi.org/10.1016/j.jmmm.2021.168611.
[5] K. Ogura, M. Takahashi, N. Nakatani, N. Ishii, Y. Miyamoto, Magnetization Analysis of Magnetic Nanowire Memory Utilizing Two Recording Metal Wires for Low Current Recording, J. Magn. Soc. Japan 46 (2022) 6-9.https://doi.org/10.3379/msjmag.2201R002.
[6] C. Li, J. Ly, B. Lei, W. Fan, D.H. Zhang, J. Han, M. Meyyappan, M. Thompson, C.W. Zhou, Data storage studies on nanowire transistors with self-assembled porphyrin molecules, J. Phys. Chem. B 108 (2004) 9646-9649. https://doi.org/10.1021/jp0498421.
[7] J. Xu, B. Hong, X. Peng, X. Wang, H. Ge, J. Hu, Preparation and magnetic properties of gradient diameter FeCoNi alloys nanowires arrays, Chem. Phys. Lett. 767 (2021) 138368. https://doi.org/10.1016/j.cplett.2021.138368.
[8] Y. Cui, I.Y. Phang, R.S. Hegde, Y.H. Lee, X.Y. Ling, Plasmonic silver nanowire structures for two-dimensional multiple-digit molecular data storage application, ACS Photonics 1 (2014) 631-637. https://doi.org/10.1021/ph5001154.
[9] M. Najafi, P. Assari, A.A. Rafati, M. Hamehvaisy, Effect of the Electrodeposition Frequency, Wave Form, and Thermal Annealing on Magnetic Properties of $[Co_{0.975}Cr_{0.025}]_{0.99}Cu_{0.01}$ Nanowire Arrays, J. Supercond. Nov. Magn. 27 (2014) 2821-2827. https://doi.org/10.1007/s10948-014-2761-3.
[10] M. Najafi, A.A. Rafati, M. Khorshidi Fart, A. Zare, Effect of the pH and electrodeposition frequency on magnetic properties of binary $Co_{1-x}Sn_x$ nanowire arrays, J. Mater. Res. 29 (2014) 190-196. https://doi.org/10.1557/jmr.2013.371.
[11] M. Najafi, Influence of Composition, pH, Annealing Temperature, Wave Form, and Frequency on Structure and Magnetic Properties of Binary $Co_{1-x}Al_x$ and Ternary $(Co_{0.97}Al_{0.03})_{1-x}Fe_x$ Nanowire Alloys, J. Supercond. Nov. Magn. 29 (2016) 2461-2471, https://doi.org/10.1007/s10948-019-05225-2.

[12] M. Najafi, P. Amjadi, Z. Alemipour, Fabrication and magnetic properties of ordered $Co_{100-x}Pb_x$ nanowire arrays electrodeposited in AAO templates: Effects of annealing temperature and frequency, J. Mater. Res. 32 (2017) 1177-1183. https://doi.org/10.1557/jmr.2017.67.
[13] Utsav, S. Khanna, S. Paneliya, N.H. Makani, I. Mukhopadhyay, R. Banerjee, Controlled restructuring of bidisperse silica nanospheres for size-selective nanowire growth, Mater. Chem. Phys. 273 (2021) 125063. https://doi.org/10.1016/j.matchemphys.2021.125063.
[14] F. Liu, P.J. Cao, H.R. Zhang, J.F. Tian, C.W. Xiao, C.M. Shen, J.Q. Li, H.J. Gao, Novel nanopyramid arrays of magnetite, Adv. Mater. 17 (2005) 1893-1897. https://doi.org/10.1002/adma.200500367.
[15] R. Pang, C. Cui, W. Yang, M. Guo, Fabrication and magnetic properties of Tb-doped multiphase Pr-Tb-Fe-B magnetic nanowire arrays, Mater. Chem. Phys. 262 (2021) 124299. https://doi.org/10.1016/j.matchemphys.2021.124299.
[16] M.U. Farooq, S. Atiq, M. Zahir, M.S. Kiani, S.M. Ramay, B. Zou, J. Zhang, Spin-polarized exciton formation in Co-doped GaN nanowires, Mater. Chem. Phys. 245 (2020) 122756. https://doi.org/10.1016/j.matchemphys.2020.122756.
[17] A. Rudolph, M. Soda, M. Kiessling, T. Wojtowicz, D. Schuh, W. Wegscheider, J. Zweck, C. Back, E. Reiger, Ferromagnetic GaAs/GaMnAs core–shell nanowires grown by molecular beam epitaxy, Nano Lett. 9 (2009) 3860–3866. https://doi.org/10.1021/nl9020717.
[18] M. Mohammadalizadeh, M. Almasi Kashi, M. Noormohammadi, Angular-dependent magnetic properties of chemically synthesized single crystalline Co nanowires, Mater. Chem. Phys. 281 (2022) 125807. https://doi.org/10.1016/j.matchemphys.2022.125807.
[19] M. Almasi Kashi, A.H. Montazer, Template-based electrodeposited nonmagnetic and magnetic metal nanowire arrays as building blocks of future nanoscale applications, J. Phys. D: Appl. Phys. 55 (2022) 233002. https://doi.org/10.1088/1361-6463/ac4d48.
[20] E. Mafakheri, P. Tahmasebi, D. Ghanbari, Application of artificial neural networks for prediction of coercivity of highly ordered cobalt nanowires synthesized by pulse electrodeposition, Measurement, 45 (6) (2012) 1387-1395. https://doi.org/10.1016/j.measurement.2012.03.027.
[21] G. Nabiyouni, N. Ahmadvand, M. Najafi, D. Ghanbari, Growth and Characterization of Iron Nanowires Into Anodized Aluminum Oxide Templates Using Electrodeposition Technique, J. Nanostructure, 9 (3) (2019) 437-441. https://doi.org/10.22052/JNS.2019.03.005
[22] L. Abbasi, K. Hedayati, D. Ghanbari, Magnetic properties and kinetic roughening study of prepared polyaniline: lead ferrite, cobalt ferrite and nickel ferrite nanocomposites electrodeposited thin films, J. Mater. Sci.: Mater. Electron., 32 (2021) 14477–14493. https://doi.osrg/10.1016/10.1007/s10854-021-06006-1
[23] G. Nabiyouni, K. Hedayati, Fabrication and magnetic study of Co/Pt multilayer nanowires and Co–Pt alloy nanowires electrodeposited into porous Si substrates, J. Exp. Nanosci. 9 (2014) 186-196. https://doi.org/10.1080/17458080.2011.654273
[24] A.H.A. Elmekawy, E. Iashina, I. Dubitskiy, S. Sotnichuk, I. Bozhev, D. Kozlov, K. Napolskii, D. Menzel, A. Mistonov, Magnetic properties of ordered arrays of iron nanowires: The impact of the length, J. Magn. Magn. Mater. 532 (2021) 167951. https://doi.org/10.1016/j.jmmm.2021.167951.
[25] H. Zhang, W. Jia, H. Sun, L. Guo, J. Sun, Growth mechanism and magnetic properties of Co nanowire arrays by AC electrodeposition, J. Magn. Magn. Mater. 468 (2018) 188-192. https://doi.org/10.1016/j.jmmm.2018.08.013.
[26] A. Vorobjova, D. Tishkevich, D. Shimanovich, T. Zubar, K. Astapovich, A. Kozlovskiy, M. Zdorovets, A. Zhaludkevich, D. Lyakhov, D. Michels, D. Vinnik, V. Fedosyuk, A. Trukhanov, The influence of the synthesis conditions on the magnetic behaviour of the densely packed arrays of Ni nanowires in porous anodic alumina membranes, RSC Adv. 11 (2003) 3952-3962. https://doi.org/10.1039/D0RA07529A.
[27] J. Xu, J. Zhang, J. Wang, B. Hong, X. Peng, X. Wang, H. Ge, J. Hu, Effects of gradient diameter on magnetic properties of FeNi alloys nanowires arrays, J. Magn. Magn. Mater. 499 (2020) 166207. https://doi.org/10.1016/j.jmmm.2019.166207.
[28] S. Aslam, A. Das, M. Khanna, B.K. Kuanr, Concentration gradient Co–Fe nanowire arrays: Microstructure to magnetic characterizations. J. Alloys Compd. 838 (2020) 155566, https://doi.org/10.1016/j.jallcom.2020.155566.
[29] N. Mansouri, N. Benbrahim-Cherief, E. Chainet, F. Charlot, T. Encinas, S. Boudinar, B. Benfedda, L. Hamadou, A. Kadri, Electrodeposition of equiatomic FeNi and FeCo nanowires: Structural and magnetic properties, J. Magn. Magn. Mater. 493 (2020) 165746. https://doi.org/10.1016/j.jmmm.2019.165746.
[30] M.S. Viqueira, G. Pozo-López, S.E. Urreta, A.M. Condó, D.R. Cornejo, L.M. Fabietti, Magnetic hysteresis in small-grained Co_xPd_{1-x} nanowire arrays, J. Magn. Magn. Mater. 394 (2015) 185-194. https://doi.org/10.1016/j.jmmm.2015.06.033.

[31] Y.W. Wang, L.D. Zhang, G.W. Meng, X.S. Peng, Y.X. Jin, J. Zhang, Fabrication of Ordered Ferromagnetic−Nonmagnetic Alloy Nanowire Arrays and their Magnetic Property Dependence on Annealing Temperature, J. Phys. Chem. B. 106 (2002) 2502–2507. https://doi.org/10.1021/jp013115d.
[32] G.B. Ji, S.L. Tang, B.X. Gu, Y.W. Du, Ordered $Co_{48}Pb_{52}$ Nanowire Arrays Electrodeposited in the Porous Anodic Alumina Oxide Template with Enhanced Coercivity, J. Phys. Chem. B. 108 (2004) 8862–8865. https://doi.org/10.1021/jp0367023.
[33] Li, H.; Xu, C.L.; Zhao, G.Y.; Li, H.L., Effects of Annealing Temperature on Magnetic Property and Structure of Amorphous $Co_{49}Pt_{51}$ Alloy Nanowire Arrays Prepared by Direct-Current Electrodeposition, J. Phys. Chem. B. 109 (2005) 3759–3763. https://doi.org/10.1021/ja806979b.
[34] X. Lin, G. Ji, T. Gao, J. Nie, Y. Du, Magnetic properties of Co–Cu nanowire arrays fabricated in different conditions by SC electrodeposition, Solid State Commun. 152 (2012) 1585-1589. https://doi.org/10.1016/j.ssc.2012.05.016.
[35] W. Lee, S.J. Park,, Porous Anodic Aluminum Oxide: Anodization and Templated Synthesis of Functional Nanostructures, Chem. Rev. 114 (2014) 7487-7556. https://doi.org/10.1021/cr500002z.
[36] M. Najafi, S. Soltanian, H. Danyali, R. Hallaj, A. Salimi, S.M. Elahi, P. Servati, Preparation of cobalt nanowires in porous aluminum oxide: Study of the effect of barrier layer, J. Mater. Res. 27 (2012) 2382-2390. https://doi.org/10.1557/jmr.2012.198.
[37] B. Astinchap, Z. Alemipour, M.J. Faraji, Effects of pH and annealing on microstructure and magnetic properties of fabricated $Co_{100-x}W_x$ nanowire arrays by AC electrodeposition, J. Magn. Magn. Mater. 498 (2020) 166245. https://doi.org/10.1016/j.jmmm.2019.166245.
[38] J.H. Gao, Q.F. Zhan, W. He, D.L. Sun, Z.H. Cheng, Synthesis and magnetic properties of Fe_3Pt nanowire arrays fabricated by electrodeposition, Appl. Phys. Lett. 86 (2005) 232506. https://doi.org/10.1063/1.1944210.
[39] R. Zhao, J.J. Gu, L.H. Liu, Q. Xu, N. Cai, H.Y. Sun, Magnetization reversal in FeCo binary alloy nanowire arrays, Acta Phys. Sin. 61 (2012) 027504. https://doi.org/10.1103/PhysRevB.66.134436.
[40] Q.F. Zhan, Z.Y. Chen, D.S. Xue, F.S. Li, H. Kunkel, X.Z. Zhou, R. Roshko, G. Williams, Structure and magnetic properties of Fe-Co nanowires in self-assembled arrays, Phys. Rev. B 66 (2002) 134436, https://doi.org/10.1088/0953-8984/16/45/027.
[41] F. Li, T. Wang, L. Ren, J. Sun, Structure and magnetic properties of Co nanowires in self-assembled arrays, J. Phys.: Condens. Matter. 16 (2004) 8053. https://doi.org/10.1088/0953-8984/16/45/027.